

Beyond Agreement: Scoring Panel-Surfaced Biomedical Entity Candidates for Curator Triage

Shuheng Cao^{1,*} Ruiqi Chen^{2,*} Renjie Cao^{3,†}
Zhenhao Zhang^{4,‡} Siyu Zhang^{1,†} Tingting Dan^{5,‡}

¹University of California, San Diego

²University of Michigan, Ann Arbor

³The Hong Kong University of Science and Technology, Guangzhou

⁴ShanghaiTech University

⁵University of North Carolina, Chapel Hill

*Equal contribution as co-first authors.

†Equal contribution.

‡Corresponding author.

Abstract

Biomedical curation turns entity mentions into review decisions. Modern LLM panels can surface plausible biomedical candidates, but multi-model agreement signals salience and does not establish corpus convention correctness. We define panel surfaced candidate verification as a curator-facing layer after candidate generation, and introduce a candidate-level panel output benchmark that aligns eight LLMs’ outputs over five public biomedical Named Entity Recognition(NER) datasets into candidate rows. We instantiate this layer with BioConCal, a supervised scorer that uses inference-time gold-free panel and candidate features to rank a candidate stream. In the in-domain document split, BioConCal raises AU-ROC from 0.753 for raw agreement to 0.910. At a validation selected 0.95 precision target, it selects 1,340 candidate rows at empirical precision 0.939, compared with 293 rows for raw agreement, with $R_{\text{cand}} = 0.592$ and row label $R_{\text{corpus}} = 0.523$ against a panel row label ceiling of 0.883. These results show that calibrated panel evidence can turn a noisy candidate stream into a higher-yield review queue, while preserving the workflow boundary that candidate sources set the recoverable universe. Target domain validation, source expansion tradeoffs, span reconciliation, and human review remain downstream requirements.

1 Introduction

Biomedical named entity recognition is often evaluated as span extraction. In curation pipelines, however, extracted mentions become review decisions. A curator must decide whether a candidate

should be accepted, routed for review, or rejected. False positives that reach a curated resource can be costly to trace and reverse (Li et al., 2016; Dogan et al., 2014; Smith et al., 2008; Collier and Kim, 2004; Krallinger et al., 2015).

Modern LLMs sharpen this decision point. They can surface plausible biomedical candidates under new entity definitions without task-specific training (Singhal et al., 2023; Luo et al., 2022; Nagar et al., 2024). Their outputs also include plausible non gold candidates, boundary variants, type confusions, and convention mismatches. The central difficulty is not only whether a phrase looks biomedical. It is whether the candidate follows the target corpus convention. We use corpus convention correctness to mean compatibility with the target dataset boundary, entity type, granularity, normalization, occurrence, and annotation rules. It does not mean independent biomedical truth verification.

Multi-model agreement is an obvious triage signal. Candidates emitted by several models are often more salient. Yet salience is not correctness under a corpus convention. The question for curation is whether a stream of candidates surfaced by a model panel can be calibrated and prioritized for curator review.

We call this problem panel surfaced candidate verification. It is a layer after candidate generation and before human curation. The input is a fixed candidate stream from a defined model panel. The output is a candidate correctness score for the curator facing triage. The unit is an aligned candidate row, not an individual LLM extractor output.

The panel defines the recoverable candidate universe, and scoring determines review yield within that universe. We therefore separate candidate-level triage from corpus-level coverage.

We instantiate this setting with a candidate-level panel output benchmark and BioConCal. The benchmark aligns eight LLMs’ outputs over five public biomedical NER datasets into candidate rows with agreement structure, inference time gold-free candidate features, and multiple correctness labels. BioConCal is an in-domain supervised scorer learned from labelled candidate rows. At inference time, it uses panel-derived signals and candidate metadata to prioritize a fixed candidate stream for review. In domain, BioConCal raises AUROC from 0.753 for raw agreement to 0.910 and selects 1,340 candidate rows at empirical precision 0.939 under the validation selected 0.95 target, compared with 293 rows for raw agreement.

We make four contributions.

1. We define panel surfaced candidate verification, a curator facing problem that starts after candidate generation and asks which surfaced candidates should be prioritized for review.
2. We construct a candidate-level panel output benchmark by aligning eight LLMs’ outputs over five public biomedical NER datasets into candidate rows with agreement structure, candidate metadata, correctness labels, and candidate universe ceilings.
3. We introduce **BioConCal**, an in-domain supervised scorer that uses inference time gold free panel and candidate features to calibrate fixed stream candidates for curator triage.
4. We analyze the workflow boundary, showing how agreement errors, validation-selected operating points, source expansion, deterministic span reconciliation, and human review shape deployment.

2 Benchmark and Candidate Construction

This benchmark evaluates candidate verification after generation. Its unit is an aligned candidate row surfaced by an explicitly defined panel. Each row represents a possible curator decision rather than a standalone extractor output.

Dataset	Entity types	Role
BC5CDR	chemical, disease	Main
NCBI Disease	disease	Main
BC2GM	gene	Main
JNLPBA	protein, DNA, RNA, cell line, cell type	Main
CHEMDNER	chemical	Robustness only

Table 1: Five biomedical NER datasets. Each contributes 500 documents to the benchmark.

2.1 Datasets

We use five biomedical NER datasets covering eight unified entity types (chemical, disease, gene, protein, DNA, RNA, cell line, cell type). Table 1 lists the datasets. Four datasets form the main benchmark. CHEMDNER is treated as robustness only for offset-sensitive analyses because the public mirror does not provide reliable character offsets. For each dataset, we sample 500 documents with a fixed random seed. This fixed-size design balances entity schemas and keeps the eight model panel evaluation tractable. The benchmark is not intended to replace full corpus extractor leaderboards. It is designed to study candidate verification under a shared panel protocol. The resulting benchmark contains 2,500 documents, and each model is evaluated on the same document identifiers, giving 20,000 model-document extraction calls.

2.2 Model panel

The panel has eight models. Two are closed frontier systems (OpenAI GPT-5.5 and Claude Opus 4.7), and six are local open weight models covering dense, MoE, instruction-tuned, and reasoning families (Meta AI, 2024; Yang et al., 2025; DeepSeek-AI, 2025; MiniMax AI, 2025; Mistral AI, 2025; Abdin et al., 2024). The panel is used as a heterogeneous candidate source rather than a leaderboard of individual LLMs. Diversity across providers and model families creates the agreement and disagreement structure used by the downstream scorer. Local serving uses vLLM with an OpenAI-compatible endpoint (Kwon et al., 2023). The full per model panel table is in Appendix Table 7.

2.3 Candidate master table

For every document, we align model predictions into occurrence-level candidate rows under (normalized_text, type) keys. Outputs assigned to the same occurrence slot are merged into one row with a vote bitmap, provider list, and

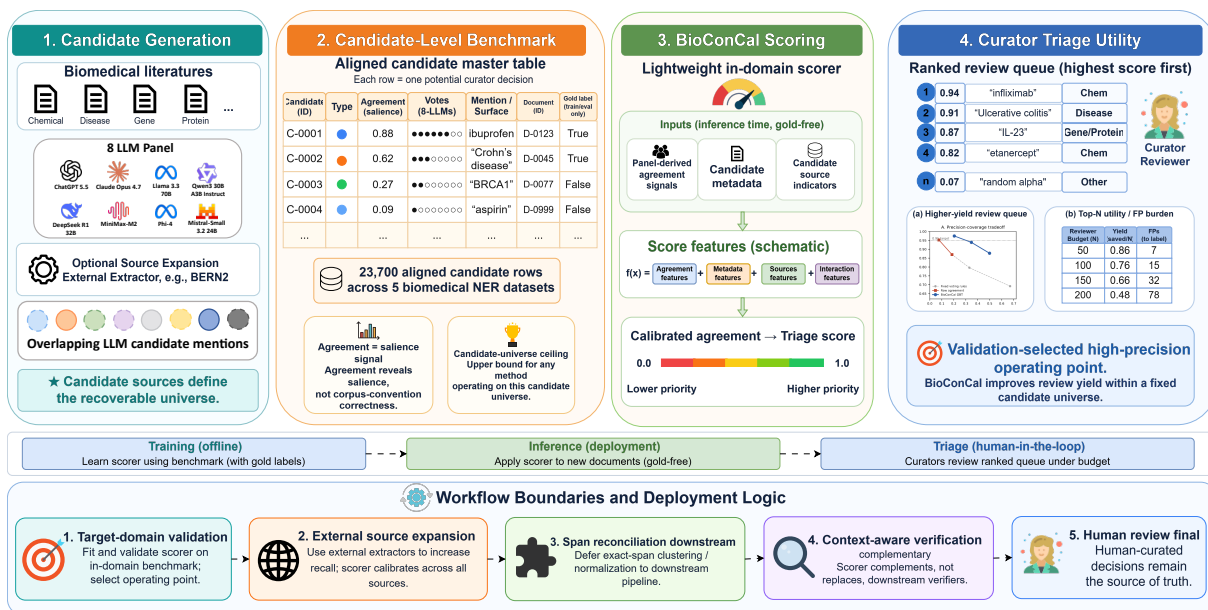


Figure 1: BioConCal overview. A multi-model panel first surfaces biomedical entity candidates, which are aligned into candidate rows for benchmark construction. BioConCal scores this fixed candidate stream using inference-time gold-free panel and candidate features, then ranks candidates for curator triage. The workflow separates candidate generation, candidate-level verification, validation-selected operating points, span reconciliation, and final human review.

surface variants.

Repeated mentions are retained as separate rows. If a document contains four mentions of the same chemical and the panel emits two surface variants, the candidate master keeps occurrence level rows rather than collapsing all evidence into one normalized string. This design matches the curator-facing unit of review.

Surface variants and provider offsets are retained for downstream analysis. Exact span labels use the first available provider offset. The `offset_available_count` and `offset_ambiguity_count` fields flag missing or many to many offset evidence for deterministic span alignment.

Multiset coverage caps repeated candidate keys at the corresponding gold occurrence count. Extra repeated candidates are overflow and cannot increase corpus recall. Gold annotations define training and evaluation labels. They are not used as input features at inference time. The resulting table has 23,700 rows and is the unit of analysis for all candidate scoring experiments.

Candidate universe. The panel defines the recoverable candidate universe. All candidate-level scoring, coverage, and selection metrics in this paper are computed over that universe. Gold mentions missed by all panel models remain outside

it. A post hoc scorer can prioritize surfaced candidates, but it cannot select candidates no source produced.

Two recall spaces. BioConCal ranks only surfaced candidates. We therefore report R_{cand} over positive candidate rows. We also report R_{corpus} over all corpus gold mentions. This second metric includes the candidate generator ceiling because gold mentions that no panel model surfaced cannot be selected by a scorer.

Two ceiling conventions distinguish triage from source comparison. The row label panel ceiling is the maximum R_{corpus} under the paper’s candidate row labels, with 2,124 positive candidate rows divided by 2,404 gold mentions, or 0.883. The stricter multiset source ceiling measures represented gold occurrences after capping repeated (`document`, `type`, `normalized_text`) keys by gold occurrence counts, giving $2,057/2,404 = 0.856$ for LLM-8. We use the stricter ceiling when comparing candidate generators such as BERN2. Sampled documents absent from the candidate master have zero gold mentions in the released samples, so the corpus denominator includes all gold mentions in the sampled test documents and is unchanged by excluding zero-candidate, zero-gold documents from candidate-row scoring.

2.4 Matching variants

We use four matching variants to separate candidate identity from localization sensitivity. **Exact span type** declares a prediction correct when document, entity type, surface text, start, and end agree. **Exact surface type** drops the offset constraint. **Normalized text type** additionally tolerates case, whitespace, and punctuation variants and is the primary candidate label. **Relaxed overlap type** additionally accepts substring containment of normalized text or overlapping offsets of the same type. BioConCal predicts the normalized text type label. Exact surface and exact span labels are used to characterize downstream localization sensitivity in Section 6.1.

Candidate keying. The keying analyses test whether the benchmark conclusions depend on row granularity or label strictness. The main benchmark uses occurrence-aware rows and normalized text-type labels. Appendix Table 21 varies row aggregation, while Appendix Table 20 varies the correctness label with the candidate set held fixed.

3 BioConCal for Candidate Triage

BioConCal is a supervised scorer for fixed panel surfaced candidate rows. For each row, it estimates correctness under the normalized text type label defined in Section 2.4. Scores rank the candidate queue for curator review within the candidate universe defined by the panel. BioConCal therefore changes review priority, not candidate generation or exact offset localization.

The input representation uses only features available at inference time. The features fall into four groups. **Agreement structure:** total, closed-model, and open-model agreement counts, plus a model-family diversity score over six families. **Mention features:** surface length, token count, document occurrence count, and binary indicators for dash, slash, parenthesis, digit, Greek letter, and capitalized abbreviation. **Surface availability:** exact and normalized surface presence in the document, plus the count and ambiguity of provider-supplied offsets. **Document features:** document length and one-hot entity type. Gold annotations define the supervised training label. Gold-derived signals such as gold entity count, hardness score, and difficulty bucket are excluded from the inputs to prevent leakage. The complete feature list is in Appendix Table 14.

We instantiate BioConCal with two standard supervised scorers. Logistic regression gives a linear treatment of standardized features. A gradient boosted tree (GBT) scorer captures nonlinear interactions using `HistGradientBoostingClassifier` with 300 iterations, learning rate 0.06, and L2 regularization 0.5. We also include isotonic regression on the raw agreement count as a single feature calibration baseline. Expected calibration error (ECE) is computed with 10 equal-width bins. Calibration refers to empirical probability scoring and validation-selected operating points. It is not a distribution-free precision guarantee.

3.1 Training and evaluation

All train, validation, and test splits are at document level. The primary in-domain protocol uses a 60/20/20 split stratified by dataset, seed 42. We assert split integrity by checking that no (dataset, doc_id) pair appears in more than one split. The check is saved in `tables/split_integrity_check.json`.

We use a leave one dataset out (LODO) protocol to separate ranking transfer from operating point transfer. In each fold, BioConCal trains on three of the four main datasets and tests on the held-out dataset. Within the training pool, documents are split 75/25 into inner training and inner validation folds. CHEMDNER remains a separate robustness setting.

Operating points are selected only on validation data. For the 0.90, 0.95, and 0.97 precision targets, thresholds are selected on the validation fold and then *frozen* before scoring the test fold. We never select thresholds on test data. We report AUROC, AUPRC, Brier score, and ECE, plus empirical test precision, test recall, selected count, and false positive count at each validation selected threshold.

4 Experimental Setup

The extraction protocol defines the candidate stream before BioConCal scoring. All panel models receive the same task instruction for a given dataset. The prompt asks each model to extract only explicitly mentioned biomedical entities from the dataset allowed type set and to return a JSON object with an `entities` array. Raw outputs are parsed into a common schema. For MiniMax-M2, Mistral-Small 3.2, and Phi-4 we use vLLM guided decoding with a JSON schema, which pre-

vents long prose reasoning and constrains output to schema-valid JSON. Missing or parse-failed rows count as zero predictions. This keeps the candidate universe tied to surfaced model outputs rather than post hoc repair.

5 Main Results

5.1 Candidate sources and agreement baselines

We report single-model scores only to characterize the panel as a heterogeneous candidate source. The objective is not to rank LLM extractors, but to study the correctness of the candidates they surface. Among single models, OpenAI gives the highest normalized mention F1 (0.800) with the highest recall, while Claude gives higher precision (0.827) at lower recall. The open-weight models occupy distinct points in the precision-recall plane, which is the diversity the agreement analysis needs. The obvious way to convert a panel into a review queue is to threshold agreement count, and this section tests that heuristic directly. Voting baselines follow the standard ensemble pattern. Union maximizes recall but admits many false positives, higher agreement thresholds raise precision and cut recall, and unanimous voting reaches the highest precision (0.940) while recovering only 11.5 percent of gold mentions. The full single-model and voting tables are in Appendix Tables 8 and 9.

5.2 Agreement is informative but incomplete

Per-mention precision rises monotonically with agreement count, from 0.266 at $k=1$ to 0.940 at $k=8$, and the largest single-step gain is between $k=1$ and $k=2$. Even unanimous agreement does not eliminate error. The unanimous set contains 1,496 predictions of which 90 are false positives, a residual rate of 6.0 percent. This is the empirical form of the deceptive-simplicity problem. A candidate can be salient enough for every model to emit, yet still violate corpus-specific correctness through boundary, type, multiplicity, or annotation-convention mismatch. We inspect these high-agreement errors in the curation-oriented audit analysis. The per- k calibration curve is in Appendix Figure 6.

5.3 Candidate scoring beyond agreement count

Learned candidate scoring converts panel agreement into a higher-yield review queue within the fixed candidate universe. Under the in-domain document-level split, BioConCal-GBT raises ranking AUROC from 0.753 for the one-feature agreement-count scorer to 0.910. It also lowers Brier score from 0.205 to 0.119. Because BioConCal scores only surfaced candidates, these gains are triage gains within the candidate universe rather than new candidate-generation recall. The full scorer comparison is in Table 3, and the operating-point comparison is in Table 2.

5.4 Validation-targeted high-precision selection

The ranking gain translates into a larger high-precision review queue. At a 0.95 precision threshold selected on the validation fold and applied frozen at test, BioConCal-GBT selects 1,340 candidates with 82 false positives and empirical test precision 0.939. Raw agreement selects 293 candidates with 14 false positives at empirical precision 0.952. Within the candidate universe, BioConCal increases recall from 0.131 to 0.592 at comparable empirical precision.

Against all corpus gold mentions, the same operating point reaches 0.523 recall in the row-label recall space, below the panel-union ceiling of 0.883. Under the stricter source-comparison accounting used for generator and hybrid analyses, the same LLM-8 operating point is reported as 0.522 in Appendix Table 27. The gain is therefore a curator-triage gain over surfaced candidates, not an end-to-end extraction recall gain. Compared with unanimity, BioConCal exposes 979 additional true candidates at the cost of 68 additional false positives. This is validation-targeted selection rather than a precision guarantee, so we report empirical test precision directly.

Monotonic transforms of the agreement count, including Platt scaling and isotonic regression, yield the same selected set as the raw agreement threshold. Split-conformal-inspired score cutoffs over the validation-fold false-positive quantile recover more candidates than raw thresholding but fall slightly below the 0.95 nominal precision on test. None of these baselines closes the precision-coverage gap achieved by BioConCal. The full table is in Appendix Table 28.

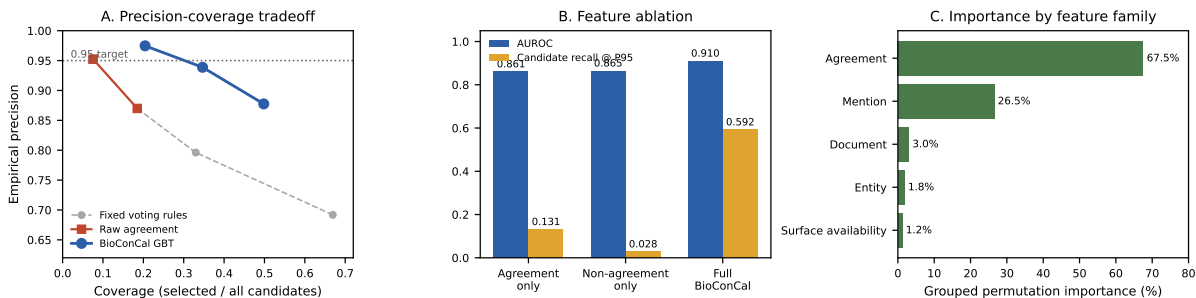


Figure 2: Why learned candidate scoring improves over agreement count, on the document-level 60/20/20 test fold. (A) BioConCal improves the raw-agreement precision-coverage tradeoff and reaches far higher coverage at the validation-frozen 0.95 precision target. (B) Agreement carries the largest signal, while candidate metadata helps convert agreement into high-yield review selection. Agreement-only and non-agreement-only scoring each recover little precision-targeted candidate recall, while the main BioConCal model reaches 0.592. (C) Grouped permutation importance. Agreement features account for 67.5 percent of grouped importance, and mention features contribute 26.5 percent. Source: `scripts/main_candidate_scoring_evidence.py`.

Method	Sel.	FP	Test P	R_{cand}	R_{corpus}	Ceil.
<i>Fixed voting rules (no threshold tuning)</i>						
Agreement ≥ 2	2,587	797	0.692	0.843	0.745	0.883
Agreement ≥ 4	1,275	260	0.796	0.478	0.422	0.883
Agreement ≥ 6	715	93	0.870	0.293	0.259	0.883
Unanimous ($k = 8$)	293	14	0.952	0.131	0.116	0.883
OpenAI \cup Claude (closed ≥ 1)	2,743	743	0.729	0.942	0.832	0.883
<i>Validation-frozen P95 threshold</i>						
Raw agreement / 8	293	14	0.952	0.131	0.116	0.883
Isotonic on agreement	293	14	0.952	0.131	0.116	0.883
BioConCal (logistic)	1,229	85	0.931	0.539	0.476	0.883
BioConCal (GBT)	1,340	82	0.939	0.592	0.523	0.883

Table 2: Validation-targeted high-precision selection on the document-level 60/20/20 test fold. Threshold-tuned methods use a 0.95 precision threshold selected on validation and applied frozen at test. R_{cand} is over 2,124 gold-positive candidate rows. R_{corpus} is over 2,404 corpus gold mentions in the row-label recall space. ‘‘Ceil.’’ is the within-panel row-label ceiling $2,124/2,404=0.883$, distinct from the stricter multiset generator-source ceiling in Appendix Table 12. Source: `tables/risk_control_selection_docsplit.csv` and `tables/end-to-end-interpretation.csv`.

5.5 Stronger candidate-scoring baselines

To test whether the gain comes from agreement count alone, vote identity alone, or candidate metadata alone, Table 3 compares progressively richer inference-time gold-free scorers under the same document-level split and validation-frozen P95 protocol.

Three controls clarify the source of the gain. Scorers built only on agreement structure, whether the 8-way vote vector or the 4 aggregate-agreement features, reach AUROC near 0.86 but recover little precision-targeted recall. The agreement pattern alone is therefore informative but insufficient for high-yield review. On the primary split, a non-agreement scorer using mention, surface, and document features reaches AUROC 0.865 but selects only 63 rows at the validation-

frozen P95 threshold. Candidate metadata alone therefore does not explain the main review-yield result.

BioConCal combines agreement and candidate metadata and reaches R_{cand} 0.592 at empirical precision 0.939. Permutation importance on the validation fold attributes about 67 percent of grouped importance to agreement features and 27 percent to mention features, with `closed_agreement_count` the strongest individual feature. The GBT and logistic forms of BioConCal are close in AUROC, 0.910 against 0.891. BioConCal is therefore best read as a panel-surfaced candidate verification framework rather than a single fixed classifier architecture.

A feature-removal ablation shows AUROC within ± 0.004 of the main BioConCal model

Scorer	AUROC	Brier	ECE	P@95	R _{cand} @95	R _{corpus} @95
Raw agreement count	0.753	0.205	0.077	0.952	0.131	0.116
Vote-vector logistic	0.864	0.148	0.059	0.941	0.151	0.134
Aggregate-agreement	0.861	0.148	0.056	0.952	0.131	0.116
Non-agreement only	0.865	0.151	0.043	0.952	0.028	0.025
BioConCal (logistic)	0.891	0.135	0.037	0.931	0.539	0.476
BioConCal (GBT)	0.910	0.119	0.032	0.939	0.592	0.523

Table 3: Stronger candidate-scoring baselines on the document-level 60/20/20 test fold. Vote-vector logistic uses the 8 per-model vote indicators. Aggregate-agreement uses the 4 agreement-structure features. Non-agreement only uses mention, surface, and document features. P@95, R_{cand}@95, and R_{corpus}@95 are at the validation-frozen P95 threshold. Source: tables/stronger_candidate_scoring_baselines_p95.csv. The complete logistic-and-GBT grid is in Appendix Table 16.

across variants that keep both agreement and non-agreement features. Only agreement-only and vote-pattern-only variants lose the high-yield selection behavior. Full ablations are in Appendix T.

5.6 Robustness across splits

Across 10 document-level splits, BioConCal-GBT remains stable and consistently outperforms raw agreement, with AUROC 0.907 ± 0.010 . A document-level bootstrap on seed 42 gives BioConCal-GBT AUROC and R_{cand} 95% intervals that do not overlap raw agreement. The full seed-wise and bootstrap results are in Appendix H.

5.7 Cheaper-panel and single-model candidate baselines

Panel size changes both scoring information and candidate coverage. We train candidate classifiers under restricted candidate universes on the same document-level 60/20/20 split and the same inference-time gold-free feature set. Each panel defines its own candidate universe by recomputing agreement features over the subset and dropping rows with zero in-panel votes. For comparability, R_{full}@95 is measured over the full eight-panel positive candidate set. Smaller panels are therefore penalized for candidates they cannot surface.

Cheaper panels recover much of the in-domain ranking AUROC, but they do not recover the same high-precision recall. Open-6 reaches AUROC 0.908 and Diverse-3 reaches 0.880, compared with 0.910 for Full-8. At the validation-frozen 0.95 precision target, single-model and closed-only pipelines reach at most 0.286 R_{full}@95. Diverse-3 reaches 0.446, while Full-8 reaches 0.592 by expanding the candidate universe. These results support cost-aware panel selection rather than a single universal panel. The appropriate panel depends on whether deployment prioritizes cost, reproducibil-

Panel	M	Cand.	AUROC	R _{full} @95
OpenAI	1	12,628	0.815	0.170
Claude	1	9,324	0.814	0.276
Best open	1	7,979	0.880	0.262
Closed-2	2	13,698	0.806	0.286
Diverse-3	3	15,156	0.880	0.446
Open-6	6	14,474	0.908	0.335
Full-8	8	18,812	0.910	0.592

Table 4: Cheap-panel baselines on the document-level test split. Cheaper panels recover much of AUROC, while the full panel gives higher high-precision recall by expanding the candidate universe. R_{full}@95 is empirical test recall over the full eight-panel positive candidate set at the validation-selected P95 operating point. Best open is MiniMax-M2. Diverse-3 is OpenAI plus MiniMax-M2 plus DeepSeek-R1. The full table with precision, FP, and coverage is in Appendix Table 25.

ity, or maximum recoverable review yield. The gain decomposition in Appendix Table 24 provides the corresponding feature-level comparison.

5.8 LODO and OOD deployment conditions

LODO separates ranking transfer from operating-point transfer. BioConCal improves mean AUROC over raw agreement, from 0.791 to 0.851 for GBT and 0.856 for logistic. At the validation-frozen P95 operating point, however, source-selected thresholds fall below the nominal precision target on average. These results argue for target-domain threshold validation before deployment. They do not imply that a small target calibration set always restores a high-yield operating point under entity-type shift. Per-fold transfer and target-domain recalibration results are in Appendix Tables 22 and 23.

Deployment. Deployment should select thresholds on target-domain validation data, report empirical precision after transfer, and use scores for triage rather than automatic insertion. The full deployment checklist is in Appendix J.

Method	AUROC	Brier	P@95	R _{cand} @95
Raw agreement / 8	0.791	0.199	0.893	0.230
Isotonic on agreement	0.791	0.226	0.893	0.230
BioConCal (logistic)	0.856	0.151	0.898	0.170
BioConCal (GBT)	0.851	0.182	0.910	0.170

Table 5: LODO macro mean across the four main datasets, with the threshold selected on the inner-validation fold and frozen at test. AUROC measures ranking transfer, while P@95 and R_{cand}@95 depend on transferring a source-selected operating point. Values are the macro means from `tables/bioconcal_lodo_nested_thresholds.csv`. Per-fold values are in Appendix Table 22.

The reliability diagram in Appendix Figure 5 shows that BioConCal predicted probabilities track empirical correctness closely on the in-domain fold.

5.9 An external extractor as a candidate source

External candidate sources raise the recoverable ceiling, but they also change the verification burden. We evaluate BERN2 (Sung et al., 2022) as an external candidate source on the same documents. Under strict multiset accounting, the ceiling is 0.856 for LLM-8, 0.737 for BERN2, and 0.901 for LLM-8 \cup BERN2.

BioConCal-Hybrid addresses scorer comparability with a learned GBT over a merged LLM-8 \cup BERN2 universe. It reaches AUROC 0.935 and AUPRC 0.948, and selects 1,847 candidate rows, including 1,716 row-label positives and 131 false positives. Under multiset corpus accounting, 1,705 selected gold occurrences over 2,404 corpus gold mentions give $R_{\text{corpus}} = 0.709$ at empirical precision 0.929. This recovers more corpus gold than the primary LLM-8 BioConCal workflow, but at lower empirical precision and with more false positives. The comparison supports the workflow decomposition. Generators set the recoverable universe, while learned verification determines review yield and false-positive burden within that universe. Full comparisons are in Appendix Tables 12 and 13.

6 Curation-Oriented Analysis

6.1 Span reconciliation after candidate triage

Candidate triage resolves normalized entity identity, but curation still requires exact character localization. We therefore treat span reconciliation as a downstream step rather than as part of the

scorer. Deterministic realignment searches exact, normalized, and supporting-span fallbacks, then chooses the match nearest the model offset. After alignment, exact-span F1 rises from 0.076 to 0.777 for OpenAI and from 0.162 to 0.708 for Claude. These gains show that candidate verification and localization are separable stages. The scorer prioritizes which normalized candidates should be reviewed, and alignment prepares selected candidates for offset-level inspection. Per-rule results are in Appendix Table 34.

6.2 Auditing agreement errors and review boundaries

Audit sheets make the residual review burden explicit. We release the 90 unanimous false positives and three disagreement audit sheets covering 758 further candidates (Appendix E). These sheets surface cases where agreement, source identity, or normalization cues may diverge from corpus convention. Their category labels are auto-suggested and are intended for follow-up annotation review, not as manually verified error labels.

Stratified calibration preserves the same broad increasing trend, with expected deviations in small dataset and entity type strata. The normalization ablation preserves the central pattern across matching variants (Appendix Figure 9 and Appendix Z). These checks define the boundary of the review workflow rather than a new automatic decision rule. BioConCal produces the ranked candidate queue, span reconciliation prepares selected normalized candidates for offset inspection, audit sheets expose cases requiring human adjudication, and source expansion changes the precision coverage tradeoff. Appendix Table 27 makes this boundary quantitative. The primary LLM-8 BioConCal workflow gives the largest high precision review yield in the LLM-8 queue, while BioConCal-Hybrid recovers more corpus gold at lower empirical precision.

7 Conclusion

We introduced a candidate-level panel output benchmark for panel surfaced candidate verification, a curator triage layer between biomedical entity extraction and human review. In the in-domain document split, BioConCal raised AUROC from 0.753 for raw agreement to 0.910. At the validation selected 0.95 precision target, it selected 1,340 candidate rows at empirical precision 0.939,

compared with 293 rows for raw agreement. This operating point gives $R_{\text{cand}} = 0.592$ and row label $R_{\text{corpus}} = 0.523$ within a panel universe whose row label ceiling is 0.883. The results support a workflow decomposition in which candidate sources set the recoverable universe, learned scoring determines review yield within that universe, and source expansion through BERN2 trades coverage for lower empirical precision. Target domain validation, deterministic span reconciliation, and human review remain required before selected candidates can support curated resource updates.

Limitations

Candidate universe and verifier scope. BioConCal scores candidates that have already been surfaced by the panel. It does not generate new mentions and cannot recover gold mentions missed by every panel model. Within panel corpus recall is therefore bounded by the row label ceiling of 0.883 on the test fold. BioConCal is also not an upper bound on context-aware verification. Richer context-aware verifiers can be used after BioConCal when a candidate needs textual evidence beyond panel and candidate metadata.

Portability and operating points. BioConCal is tied to the candidate sources, prompts, decoding constraints, corpus convention, and entity type mix used to train and validate it. If any of these change, the classifier and its operating threshold require target domain validation before deployment. The LODO and target recalibration analyses show why this validation matters under entity type shift, but they do not guarantee that 25 to 100 labeled documents will recover the same yield in every target corpus. Prompt sensitivity is evaluated on an open weight subset in Appendix X.

Human review and reproducibility. BioConCal scores define a review priority, not automatic acceptance or rejection. False positives can contaminate curated biomedical resources if accepted without review, and false negatives can leave useful candidates outside the high-priority queue. High scores, low scores, and audit categories should therefore be treated as triage signals for human adjudication. The released audit categories are auto-suggested and are intended to guide follow-up review rather than serve as verified error labels. Closed API providers introduce cost and reproducibility asymmetry, while

the open weight six model variant is the reproducible alternative. CHEMDNER is kept as a robustness dataset because its public mirror lacks reliable character offsets. We report empirical test precision and do not claim distribution-free precision guarantees.

Ethics and Reproducibility

All datasets are public biomedical NER resources, and the work introduces no new human-subject data. We release all analysis scripts, and the open-weight six-model variant is locally reproducible. The full eight-model benchmark depends on closed API access. Reproduction commands are in Appendix A.

References

- Marah Abdin, Jyoti Aneja, Harkirat Behl, Sebastien Bubeck, Ronen Eldan, Suriya Gunasekar, Michael Harrison, Russell J. Hewett, Mojan Javaheripi, Piero Kauffmann, and 1 others. 2024. Phi-4 technical report. *arXiv preprint arXiv:2412.08905*.
- Anastasios N. Angelopoulos and Stephen Bates. 2021. A gentle introduction to conformal prediction and distribution-free uncertainty quantification. In *arXiv preprint*. Preprint.
- Nigel Collier and Jin-Dong Kim. 2004. Introduction to the bio-entity recognition task at jnlpba. In *Proceedings of the International Joint Workshop on Natural Language Processing in Biomedicine and its Applications*, pages 73–78.
- Udiptaman Das, Krishnasai B. Atmakuri, Duy Ho, Chi Lee, and Yugyung Lee. 2026. Clinical knowledge graph construction and evaluation with multi-llms via retrieval-augmented generation. *ArXiv preprint arXiv:2601.01844*.
- Rodrigo de Oliveira, Matthew Garber, James M. Gwinnett, Emaan Rashidi, Jwu-Hsuan Hwang, William Gilmour, Jay Navavati, Khaldoun Zine El Abidine, and Christina DeFilippo Mack. 2025. [A study of calibration as a measurement of trustworthiness of large language models in biomedical natural language processing](#). *JAMIA Open*, 8(4):ooaf058.
- DeepSeek-AI. 2025. Deepseek-r1: Incentivizing reasoning capability in llms via reinforcement learning. *arXiv preprint arXiv:2501.12948*.
- Thomas G. Dietterich. 2000. Ensemble methods in machine learning. In *Multiple Classifier Systems*, pages 1–15. Springer.
- Rezarta Islamaj Dogan, Robert Leaman, and Zhiyong Lu. 2014. [Ncbi disease corpus: a resource for disease name recognition and concept normalization](#). *Journal of Biomedical Informatics*, 47:1–10.

- Jason Fries, Natasha Seelam, Gabriel Altay, Leon Weber, Myungsun Kang, Debajyoti Datta, Ruisi Su, Samuele Garda, Bo Wang, Simon Ott, Matthias Samwald, and Wojciech Kusa. 2022. [Dataset debt in biomedical language modeling](#). In *Proceedings of BigScience Episode #5 – Workshop on Challenges & Perspectives in Creating Large Language Models*, pages 137–145, virtual+Dublin. Association for Computational Linguistics.
- Yonatan Geifman and Ran El-Yaniv. 2017. Selective classification for deep neural networks. In *Advances in Neural Information Processing Systems*.
- Yu Gu, Robert Tinn, Hao Cheng, Michael Lucas, Naoto Usuyama, Xiaodong Liu, Tristan Naumann, Jianfeng Gao, and Hoifung Poon. 2021. [Domain-specific language model pretraining for biomedical natural language processing](#). *ACM Transactions on Computing for Healthcare*, 3(1):1–23.
- Anshita Khandelwal, Alok Kar, Veera Raghavendra Chikka, and Kamalakar Karlapalem. 2022. [Biomedical NER using novel schema and distant supervision](#). In *Proceedings of the 21st Workshop on Biomedical Language Processing*, pages 155–160, Dublin, Ireland. Association for Computational Linguistics.
- Martin Krallinger, Obdulia Rabal, Florian Leitner, Miguel Vazquez, David Salgado, Zhiyong Lu, Robert Leaman, and 1 others. 2015. [The chemdner corpus of chemicals and drugs and its annotation principles](#). *Journal of Cheminformatics*, 7(Suppl 1):S2.
- Woosuk Kwon, Zhuohan Li, Siyuan Zhuang, Ying Sheng, Lianmin Zheng, Cody Hao Yu, Joseph E. Gonzalez, Hao Zhang, and Ion Stoica. 2023. [Efficient memory management for large language model serving with pagedattention](#). In *Proceedings of the 29th Symposium on Operating Systems Principles*, pages 611–626.
- Jinhyuk Lee, Wonjin Yoon, Sungdong Kim, Donghyeon Kim, Sunkyu Kim, Chan Ho So, and Jaewoo Kang. 2020. [Biobert: a pre-trained biomedical language representation model for biomedical text mining](#). *Bioinformatics*, 36(4):1234–1240.
- Jiao Li, Yueping Sun, Robin J. Johnson, Daniela Sciaky, Chih-Hsuan Wei, Robert Leaman, Allan Peter Davis, Carolyn J. Mattingly, Thomas C. Wieggers, and Zhiyong Lu. 2016. [Biocreative v cdr task corpus: a resource for chemical disease relation extraction](#). *Database*, 2016:baw068.
- Zhen Lin, Shubhendu Trivedi, and Jimeng Sun. 2023. [Generating with confidence: Uncertainty quantification for black-box large language models](#). ArXiv preprint arXiv:2305.19187.
- Renqian Luo, Liai Sun, Yingce Xia, Tao Qin, Sheng Zhang, Hoifung Poon, and Tie-Yan Liu. 2022. [Biogpt: generative pre-trained transformer for biomedical text generation and mining](#). *Briefings in Bioinformatics*, 23(6):bbac409.
- Tengxiao Lv, Ling Luo, Juntao Li, Yanhua Wang, Yuchen Pan, Chao Liu, Yanan Wang, Yan Jiang, Huiyi Lv, Yuanyuan Sun, Jian Wang, and Hongfei Lin. 2025. [A unified biomedical named entity recognition framework with large language models](#). ArXiv preprint arXiv:2510.08902.
- Meta AI. 2024. [Llama 3.3 70b instruct](#). Hugging Face model card.
- MiniMax AI. 2025. [Minimax-m2](#). GitHub repository.
- Mistral AI. 2025. [Mistral small 3.2](#). Model card.
- Aishik Nagar, Viktor Schlegel, Thanh-Tung Nguyen, Hao Li, Yuping Wu, Kuluhan Binici, and Stefan Winkler. 2024. [Llms are not zero-shot reasoners for biomedical information extraction](#). ArXiv preprint arXiv:2408.12249.
- Alexandru Niculescu-Mizil and Rich Caruana. 2005. [Predicting good probabilities with supervised learning](#). *Proceedings of the 22nd International Conference on Machine Learning (ICML)*, pages 625–632.
- Curtis G. Northcutt, Lu Jiang, and Isaac L. Chuang. 2021. [Confident learning: Estimating uncertainty in dataset labels](#). In *Journal of Artificial Intelligence Research*, volume 70, pages 1373–1411.
- Motasem S. Obeidat, Md Sultan Al Nahian, and Ramakanth Kavuluru. 2025. [Do LLMs surpass encoders for biomedical NER?](#) In *2025 IEEE International Conference on Healthcare Informatics (ICHI)*, pages 352–358.
- John Platt. 1999. Probabilistic outputs for support vector machines and comparisons to regularized likelihood methods. *Advances in Large Margin Classifiers*, 10(3):61–74.
- Karan Singhal, Shekoofeh Azizi, Tao Tu, S. Sara Mahdavi, Jason Wei, Hyung Won Chung, Nathan Scales, Ajay Tanwani, Heather Cole-Lewis, Stephen Pfohl, and 1 others. 2023. [Large language models encode clinical knowledge](#). *Nature*, 620:172–180.
- Larry Smith, Lorraine K. Tanabe, Rie Johnson Ando, Cheng-Ju Kuo, I-Fang Chung, Chun-Nan Hsu, Yu-Shi Lin, Roman Klinger, Christoph M. Friedrich, Kuzman Ganchev, and 1 others. 2008. [Overview of biocreative ii gene mention recognition](#). *Genome Biology*, 9(Suppl 2):S2.
- Mujeen Sung, Minbyul Jeong, Yonghwa Choi, Donghyeon Kim, Jinhyuk Lee, and Jaewoo Kang. 2022. [Bern2: an advanced neural biomedical named entity recognition and normalization tool](#). *Bioinformatics*, 38(20):4837–4839.
- Swabha Swayamdipta, Roy Schwartz, Nicholas Lourie, Yizhong Wang, Hannaneh Hajishirzi, Noah A. Smith, and Yejin Choi. 2020. [Dataset cartography: Mapping and diagnosing datasets with training dynamics](#). In *Proceedings of the 2020 Conference on Empirical Methods in Natural Language Processing (EMNLP)*.

Katherine Tian, Eric Mitchell, Allan Zhou, Archit Sharma, Rafael Rafailov, Huaxiu Yao, Chelsea Finn, and Christopher D. Manning. 2023. Just ask for calibration: Strategies for eliciting calibrated confidence scores from language models fine-tuned with human feedback. ArXiv preprint arXiv:2305.14975.

Xuezhi Wang, Jason Wei, Dale Schuurmans, Quoc Le, Ed Chi, Sharan Narang, Aakanksha Chowdhery, and Denny Zhou. 2023. Self-consistency improves chain of thought reasoning in language models. In *International Conference on Learning Representations*.

Taiki Watanabe, Tomoya Ichikawa, Akihiro Tamura, Tomoya Iwakura, Chunpeng Ma, and Tsuneo Kato. 2022. Auxiliary learning for named entity recognition with multiple auxiliary biomedical training data. In *Proceedings of the 21st Workshop on Biomedical Language Processing*, pages 130–139, Dublin, Ireland. Association for Computational Linguistics.

An Yang, Anfeng Li, Baosong Yang, Beichen Zhang, Binyuan Hui, Bo Zheng, Bowen Yu, and 1 others. 2025. Qwen3 technical report. *arXiv preprint arXiv:2505.09388*.

Mingyue Yuan, Jieshan Chen, Zhenchang Xing, Gelareh Mohammadi, and Aaron Quigley. 2025. A case study of scalable content annotation using multi-llm consensus and human review. GenAICHI Workshop at CHI 2025; arXiv:2503.17620.

Youliang Yuan, Wenxuan Wang, Qingshuo Guo, Yiming Xiong, Chihao Shen, and Pinjia He. 2024. Does chatgpt know that it does not know? evaluating the black-box calibration of chatgpt. In *Proceedings of the 2024 Joint International Conference on Computational Linguistics, Language Resources and Evaluation (LREC-COLING 2024)*, pages 5191–5201.

A Reproducibility commands

The candidate master and downstream analysis tables can be regenerated from the released sample documents, parsed provider outputs, consensus candidate artifacts, and table sources. Full extraction regeneration additionally requires rerunning the provider calls; the downstream scripts below are run from the project root.

`build_candidate_master.py`: candidate-level master.
`train_bioconcal.v3.py`: doc-level 60/20/20 + LODO with inner-val thresholds.
`selective_baselines.py`: selective and conformal baselines.
`panel_composition_ablation.py`: panel ablations.
`feature_importance.py`: permutation importance + figure.
`span_alignment_audit_sample.py`: 100-row span audit sample.
`extended_span_alignment.py`: span alignment metrics.
`audit_unanimous_fps.py`: unanimous FP audit sheet (multiset).
`finalize_unanimous_fp_audit.py`: refined audit with subcategories.
`disagreement_audit.py`: candidate audit sheets.
`agreement_calibration_by_strata.py`: per-stratum.
`normalization_ablation.py`: normalization deltas.
`stronger_candidate_scoring_baselines.py`: consolidated stronger-baseline table.
`main_candidate_scoring_evidence.py`: 3-panel main evidence figure.
`train_hybrid_candidate_scorer.py`: learned LLM-8 \cup BERN2 candidate scorer.

Script locations are mixed by design. The candidate-master, training, ablation, and audit-generation scripts live under `paper_experiment_materials/strong_accept/scripts/`. The unanimous-audit finalization, stratum calibration, main evidence, stronger-baseline, and hybrid-scoring scripts live under top-level `scripts/`.

B Related work, model panel, and baseline tables

Biomedical NER and LLM candidate generation. Public biomedical NER benchmarks cover chemical, disease, gene, protein, nucleic acid, cell line, and cell type mentions (Li et al., 2016; Dogan et al., 2014; Smith et al., 2008; Collier and Kim, 2004; Krallinger et al., 2015). Biomedical encoders and generative biomedical language models include BioBERT, PubMedBERT, and BioGPT (Lee et al., 2020; Gu et al., 2021; Luo et al., 2022). Supervised biomedical NER work studies multi-dataset auxiliary learning, discontinuous and overlapping entities, and dataset availability debt (Watanabe et al., 2022; Khandelwal et al., 2022; Fries et al., 2022). Established systems combine neural recognition with entity normalization, and BERN2 (Sung et al., 2022) is a widely used biomedical NER and normalization reference point. LLM-based biomedical information extraction has been studied for zero-shot biomedical reasoning (Nagar et al., 2024), LLM versus encoder biomedical NER tradeoffs (Obeidat et al., 2025), flat and nested NER under generative frameworks

(Lv et al., 2025), and multi-LLM workflows for clinical knowledge graph construction (Das et al., 2026). These works ask whether an extractor or generator can produce entity predictions under a task schema. We start after candidate sources have produced candidates and evaluate aligned candidate rows as review decisions.

Panel-surfaced verification for curator review.

Multi LLM consensus paired with selective human review has been studied as an annotation pattern (Yuan et al., 2025). BioConCal studies a different workflow layer. Given a fixed stream of candidates surfaced by a multi-model panel, the question is whether those candidates can be ranked for curator review using agreement structure and inference time gold-free candidate features. External extractors such as BERN2 can expand the candidate universe, but they do not remove the need for source-specific verification. Context-aware verification uses richer document evidence to adjudicate individual candidates. It is complementary to the panel-derived triage layer studied here, which first ranks a large candidate stream for review. Appendix Table 6 contrasts evaluation units across related settings.

Agreement, calibration, and LLM uncertainty.

Ensembles and self-consistency are widely used to improve reliability (Dietterich, 2000; Wang et al., 2023). Probabilistic calibration of classifier outputs is standard (Platt, 1999; Niculescu-Mizil and Caruana, 2005). Selective classification allows abstention on low confidence inputs (Geifman and El-Yaniv, 2017), conformal prediction provides distribution-free coverage guarantees (Angelopoulos and Bates, 2021), and confident learning and dataset cartography use disagreement to identify possibly mislabeled examples (Northcutt et al., 2021; Swayamdipta et al., 2020). For single-LLM uncertainty, Lin et al. (2023) quantifies black-box uncertainty via the semantic dispersion of sampled generations, and Tian et al. (2023) elicits verbalized confidence from RLHF-fine-tuned LLMs. In biomedical NLP, de Oliveira et al. (2025) reports that out-of-the-box LLM calibration is poor while post hoc calibration helps, and Yuan et al. (2024) documents systematic overconfidence in the black-box calibration of a closed LLM. Our work treats multi-LLM agreement as panel evidence of salience and learns a downstream scorer from agreement and candidate metadata. It targets validation-selected operating points

for review triage rather than distribution-free guarantees or automatic curation.

C BERN2 NER reference point

We run the BERN2 NER model (the recognition component of BERN2, without entity normalization) on the same 500-document-per-dataset samples, using the official `multi_ner` module with the released `dmis-lab/bern2-ner` weights. BERN2 heads map to our schema as disease, drug to chemical, gene, DNA, RNA, cell line, and cell type, while species and mutation are ignored. BERN2 merges gene and protein into one head, so BC5CDR, NCBI Disease, and BC2GM use clean mappings while JNLPBA protein is approximate and reported separately. Table 10 reports normalized mention P/R/F1 and Table 11 the candidate-source overlap. Run details are in `bern2_run_report.md`.

Table 12 decomposes the pipeline into candidate-generation ceiling and triage yield on the same document-level test fold. The eight-LLM panel reaches strict multiset ceiling 0.856, BERN2 alone reaches 0.737, and the additive generator union reaches 0.901 by surfacing gold mentions the panel misses. The union row in Table 12 is an exploratory merge rule, not a learned scorer over a shared representation. Table 13 therefore adds BioConCal-Hybrid, a learned GBT over the merged $\text{LLM-8} \cup \text{BERN2}$ universe with LLM agreement features where available, BERN2 source indicators, and BERN2 confidence scores.

D Feature definitions

E Auto-suggested audit sheets

We release four candidate audit sheets. Set A is the unanimous false-positive list (90 candidates under multiset normalized matching). Set B is high-agreement false positives with $k \in \{6, 7\}$ (358 candidates). Set C is minority true positives with $k \leq 2$ (200 sampled). Set D is closed-versus-open disagreement (200 sampled). All sheets are CSV with auto-suggested category labels and are released to support follow-up annotation review; the categories have not been manually verified. The final Set A source is the revision file `unanimous_fp_audit_final.csv`; older combined audit artifacts are not used for the final 90-candidate count. A 100-row span-alignment audit sample stratified

Line of work	Unit of prediction	Main objective	Panel agr.	Triage score	Relation to BioConCal	
BERN2 (Sung et al., 2022)	Mention span	End-to-end NER and normalization	No	No	Candidate source	
Biomedical BERT and PubMedBERT NER (Lee et al., 2020; Gu et al., 2021)	Token and span	Supervised biomedical NER	No	No	Candidate source	
Extractor-level evaluation	NER	Model or span	Rank or score standalone extractors	No	No	Different layer
Multi-LLM consensus annotation (Yuan et al., 2025)	Item label	Consensus plus human review	Yes (count)	No	Related, count only	
BioConCal (this work)	Panel-surfaced candidate	Validation-targeted candidate triage	Yes	Yes	This work	

Table 6: Evaluation units across related settings. BioConCal conditions on surfaced candidates and evaluates candidate-level triage rather than end-to-end extraction. “Panel agr.” is whether the method uses multi-LLM panel agreement structure, and “Triage score” is whether it emits a validation-targeted candidate-correctness score.

Model	Access	Type and size
GPT-5.5	Closed API	frontier, undisclosed
Claude Opus 4.7	Closed API	frontier, undisclosed
Llama 3.3 70B	Local	open-weight dense, 70B
Qwen3-30B-A3B-Instruct	Local	open-weight MoE, 30.5B/3.3B active
DeepSeek-R1 32B	Local	open-weight reasoning, 32B
MiniMax-M2	Local	open-weight MoE, 230B/10B active
Mistral-Small 3.2 24B	Local	open-weight dense, 24B
Phi-4	Local	open-weight dense, 14B

Table 7: Eight-model panel. Six models are served locally with vLLM.

Model	P	R	F1
OpenAI GPT-5.5	0.788	0.812	0.800
Claude Opus 4.7	0.827	0.629	0.715
MiniMax-M2	0.665	0.433	0.525
Mistral-Small 3.2	0.659	0.386	0.487
Qwen3-30B-A3B	0.612	0.361	0.454
DeepSeek-R1 32B	0.743	0.319	0.446
Phi-4	0.666	0.307	0.420
Llama 3.3 70B	0.731	0.283	0.408

Table 8: Single-model normalized mention F1, overall micro on the four main datasets (excludes CHEMD-NER).

Rule	P	R	F1
Union, any model	0.573	0.880	0.694
OpenAI \cup Claude	0.763	0.854	0.806
Agreement ≥ 2	0.711	0.753	0.731
Agreement ≥ 4	0.805	0.428	0.559
Agreement ≥ 6	0.878	0.263	0.405
Unanimous ($k = 8$)	0.940	0.115	0.205

Table 9: Voting baselines on the 8-model panel. The closed-only union is the best F1 voting rule, but unanimous voting trades almost all recall for precision.

Dataset	P	R	F1
BC5CDR	0.874	0.772	0.820
NCBI Disease	0.869	0.875	0.872
BC2GM	0.864	0.868	0.866
Overall (clean)	0.873	0.782	0.825
JNLPBA (approx.)	0.509	0.740	0.603

Table 10: BERN2 NER model, normalized mention matching on the sampled documents. Overall is over BC5CDR, NCBI Disease, and BC2GM with clean type mappings. JNLPBA is approximate because BERN2 merges gene and protein. Source: tables/bern2-reference-results.csv.

across repeated-surface, multi-candidate-span, long-or-nested, overlap, and random cases is in audit/span_alignment_manual_audit_sample.csv.

F Span-alignment method success rates

G Full feature ablation

H Robustness: splits, bootstrap, and candidate keying

H.1 Per-seed and bootstrap detail

Table 18 gives the per-seed results for the headline scorer behind the summary in Table 17. Table 19 gives the document-level bootstrap 95% confidence intervals on the seed-42 test fold (2,000 resamples of documents, stratified by dataset; documents rather than candidates are resampled because within-document candidates are correlated). Both are produced without rerunning extraction, from candidate_master.csv.

I Candidate keying ablation

Dataset	Gold	Panel covered	BERN2 covered	Panel ceiling	Panel+BERN2 ceiling
BC5CDR	9,965	9,117	8,307	0.915	0.939
NCBI Disease	506	460	446	0.909	0.953
BC2GM	636	499	556	0.785	0.936
JNLPBA	1,140	1,046	848	0.918	0.930

Table 11: Candidate-source overlap. “Panel covered” and “BERN2 covered” are gold mentions whose normalized key is surfaced by each source. Adding BERN2 to the panel raises the candidate-universe ceiling, most on BC2GM genes. Source: `tables/bern2_candidate_source_overlap.csv`.

Candidate source	Cands	Repr. gold	Ceiling	Src F1	Scorer	AUROC	P@0.95	R _{cand}	R _{corpus}
LLM-8 only	3866	2057	0.856	–	BioConCal	0.910	0.939	0.592	0.522
BERN2 only	2199	1772	0.737	0.770	take-all	n/a	0.806	n/a	0.737
LLM-8 \cup BERN2	6065	2166	0.901	–	merge	n/a	0.836	n/a	0.550
Diverse-3 only	2968	1207	0.502	–	BioConCal	0.880	0.944	0.490	0.269
Diverse-3 \cup BERN2	5167	1974	0.821	–	merge	n/a	0.680	n/a	0.567

Table 12: Candidate-generator comparison on the document-level test fold (seed 42). The generator fixes the candidate-universe *ceiling* (Repr. gold = multiset gold occurrences covered; ceiling = Repr./2404); BioConCal determines *triage yield* (AUROC, P@0.95, R_{cand}, R_{corpus}) within that universe. Scorers are not forced to match: a single extractor has no agreement features, so BERN2-only is take-all (no triage) and union rows use an exploratory merge rule. “Src F1” is take-all extractor F1 on the test fold (single extractors only; “–” for panels, which have no single operating point). R_{corpus} is comparable across all rows; R_{cand} is within-universe and reported only for BioConCal-scored panels. JNLPBA gene/protein mapping is approximate. Source: `scripts/main_candidate_generator_comparison.py`, `tables/main_candidate_generator_comparison.csv`.

Workflow	Cand. source	Cands	Repr.	Ceiling	AUROC	AUPRC	Test P	Sel.	Row TP	FP	R _{corpus}	Fit
LLM-8 BioConCal	LLM-8	3,866	2,057	0.856	0.910	n/a	0.939	1,340	1,258	82	0.522	Primary
BERN2 take-all	BERN2	2,199	1,772	0.737	n/a	n/a	0.806	2,199	1,772	427	0.737	Unfiltered
LLM-8 \cup BERN2 merge	additive union	6,065	2,166	0.901	n/a	n/a	0.836	1,583	1,323	260	0.550	Unfiltered
BioConCal-Hybrid	merged union	4,140	2,150	0.894	0.935	0.948	0.929	1,847	1,716	131	0.709	Tradeoff

Table 13: Learned hybrid candidate scoring on the document-level test fold. BioConCal-Hybrid trains a GBT over a merged LLM-8 \cup BERN2 candidate universe; BERN2-only rows have zero LLM votes and source indicators mark them as BERN2-only, while overlap rows retain LLM features and receive BERN2 indicators. Row TP counts selected candidate rows labeled positive. R_{corpus} uses multiset corpus accounting; for the hybrid row, 1,705 selected multiset gold mentions over 2,404 corpus gold mentions gives R_{corpus} = 0.709. The hybrid reduces the false-positive burden relative to the exploratory merge and recovers more true candidate rows than LLM-only BioConCal, but its empirical precision 0.929 is lower than the primary LLM-8 BioConCal precision of 0.939. This is a candidate-triage comparison, not a claim that BioConCal is a better extractor than BERN2. Source: `scripts/train_hybrid_candidate_scorer.py`, `tables/hybrid_candidate_scorer_results.csv`.

Feature	Group	Definition
<code>agreement_count</code>	Agreement	Number of providers (of 8) emitting the same (normalized text, type) key.
<code>closed_agreement_count</code>	Agreement	Subcount over closed-API providers (OpenAI, Claude).
<code>open_agreement_count</code>	Agreement	Subcount over six open-weight providers.
<code>model_family_diversity_score</code>	Agreement	Distinct families among agreeing providers (six families).
<code>mention_length_chars</code>	Mention	Character length of predicted surface.
<code>mention_token_count</code>	Mention	Whitespace-token count of predicted surface.
<code>mention_occurrences_in_doc</code>	Mention	Literal occurrences of predicted surface in the source document.
<code>has_*_indicators</code>	Mention	Dash, slash, paren, digit, Greek letter, or capitalized abbreviation in the surface.
<code>exact_surface_in_doc</code>	Surface availability	1 if predicted surface is a literal substring of the document.
<code>normalized_in_doc</code>	Surface availability	1 if normalized surface is a substring of normalized document.
<code>offset_available_count</code>	Surface availability	Providers that supplied a numeric offset.
<code>offset_ambiguity_count</code>	Surface availability	Distinct (start, end) tuples across providers.
<code>doc_text_length</code>	Document	Character length of source document.
<code>entity_type</code>	Entity	Unified eight-type schema, one-hot encoded.

Table 14: BioConCal gold-free input-feature definitions. Training labels come from gold annotations and are not listed here. Per-feature permutation importance is in Figure 4.

Alignment method	Total	With gold	Post=Gold	Rate
Exact surface match	12,628	12,402	9,637	0.777

Table 15: Span-alignment method success rates on OpenAI predictions across the four main datasets. Source: tables/span_alignment_error_modes.v2.csv.

Features	Clf.	#feat.	AUROC	Brier	ECE	P@95	R _{cand} @95	Sel
A. agreement_count only	logistic	1	0.753	0.205	0.077	0.952	0.131	293
A. agreement_count only	GBT	1	0.751	0.199	0.050	0.952	0.131	293
B. vote-pattern only (8 indicators)	logistic	8	0.864	0.148	0.059	0.941	0.151	341
B. vote-pattern only (8 indicators)	GBT	8	0.859	0.151	0.053	0.953	0.143	318
C. aggregate agreement only (4 feats)	logistic	4	0.861	0.148	0.056	0.952	0.131	293
C. aggregate agreement only (4 feats)	GBT	4	0.860	0.149	0.054	0.000	0.000	0
D. non-agreement only (15 feats)	logistic	15	0.829	0.169	0.054	0.913	0.158	367
D. non-agreement only (15 feats)	GBT	15	0.865	0.151	0.043	0.952	0.028	63
E. agg. agree. + non-agree.	logistic	19	0.891	0.135	0.037	0.931	0.539	1,229
E. agg. agree. + non-agree.	GBT	19	0.910	0.119	0.032	0.939	0.592	1,340
F. vote-pattern + non-agreement	logistic	23	0.892	0.134	0.036	0.930	0.545	1,245
F. vote-pattern + non-agreement	GBT	23	0.908	0.120	0.037	0.939	0.554	1,253
G. all-feature diagnostic	logistic	27	0.892	0.134	0.037	0.928	0.540	1,237
G. all-feature diagnostic	GBT	27	0.910	0.119	0.026	0.946	0.557	1,251

Table 16: Complete feature-ablation grid (logistic + GBT, all seven feature sets). Row E is the main 19-feature BioConCal definition used in the paper; row G is an all-feature diagnostic that additionally includes the 8 per-model vote indicators. Row C-GBT (aggregate-agreement-only, GBT) selects zero candidates at the val-frozen P95 threshold because the GBT predicted-probability distribution on aggregate-agreement-only features has no validation point above the 0.95 precision target; this is a quirk of finite-sample threshold selection on a low-dimensional GBT and is included for completeness. Source: tables/feature_ablation_baselines.csv.

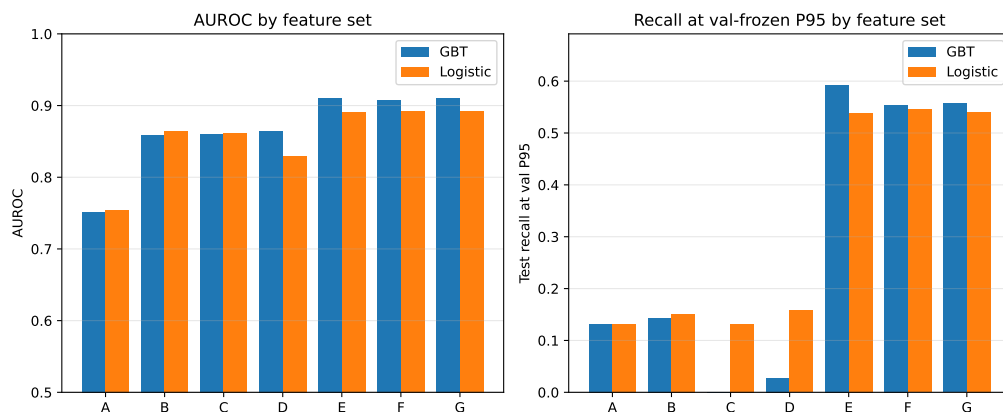


Figure 3: Feature-ablation AUROC (left) and recall at the validation-frozen P95 threshold (right) for GBT and logistic classifiers.

Scorer	AUROC	P@0.95	R _{cand} @0.95	Sel.	FP
Raw agreement count	0.742±0.010	0.931±0.034	0.149±0.044	356±114	28±23
Isotonic on agreement	0.741±0.010	0.931±0.034	0.149±0.044	356±114	28±23
Vote-vector logistic	0.852±0.011	0.898±0.077	0.043±0.076	102±176	9±16
Aggregate-agreement scorer	0.846±0.010	0.935±0.029	0.144±0.035	340±88	24±17
Non-agreement scorer	0.875±0.010	0.953±0.014	0.373±0.144	870±349	42±25
BioConCal logistic	0.895±0.010	0.948±0.017	0.471±0.049	1096±116	59±24
BioConCal GBT	0.907±0.010	0.944±0.013	0.565±0.064	1321±161	75±25

Table 17: Robustness over 10 document-level splits (seeds 13, 21, 42, 87, 101, 7, 123, 256, 512, 1000), mean±sd. Same protocol, gold-free features, and validation-targeted 0.95 precision as Table 3; each seed's recall denominators are recomputed for its own test fold. Source: scripts/repeated_docsplit_bioconcal.py, tables/repeated_docsplit_summary.csv.

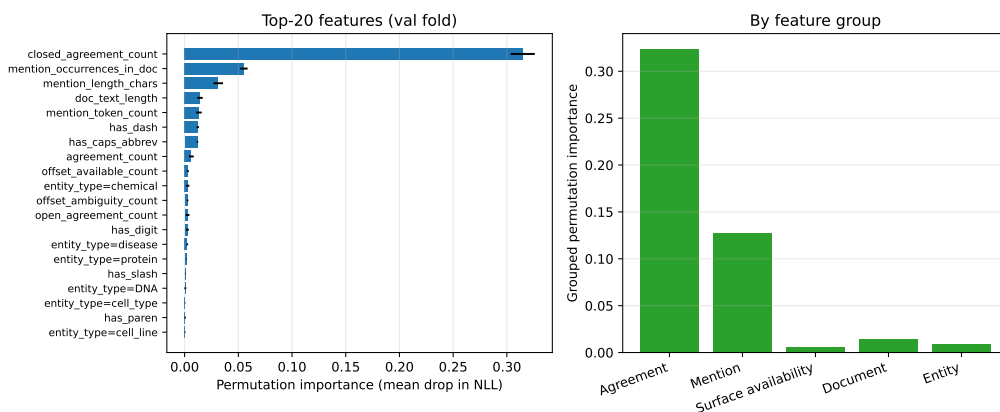


Figure 4: Permutation feature importance for BioConCal-GBT, doc-level validation fold (mean drop in negative log-loss, five shuffles). Left: top-20 individual features. Right: grouped importance by feature family.

Seed	AUROC	P@0.95	R _{cand}	R _{corpus}	Sel.	FP
7	0.915	0.935	0.635	0.579	1470	96
13	0.926	0.973	0.521	0.479	1134	31
21	0.907	0.948	0.508	0.459	1244	65
42	0.910	0.939	0.592	0.523	1340	82
87	0.914	0.938	0.647	0.586	1514	94
101	0.903	0.953	0.519	0.464	1204	57
123	0.906	0.953	0.475	0.438	1158	55
256	0.900	0.928	0.654	0.592	1578	113
512	0.890	0.944	0.528	0.475	1177	66
1000	0.900	0.932	0.574	0.515	1392	94
mean±sd	0.907±0.010	0.944±0.013	0.565±0.064	0.511±0.057	1321±161	75±25

Table 18: Per-seed BioConCal-GBT results over the 10 document-level splits. Source: `scripts/repeated_docsplit_bioconcal.py, tables/repeated_docsplit_all_seeds.csv`.

Scorer	AUROC [95% CI]	P@0.95 [95% CI]	R _{cand} [95% CI]
Raw agreement count	0.753 [0.732, 0.776]	0.952 [0.928, 0.974]	0.131 [0.112, 0.151]
Vote-vector logistic	0.864 [0.844, 0.884]	0.941 [0.914, 0.965]	0.151 [0.131, 0.174]
Aggregate-agreement scorer	0.861 [0.840, 0.880]	0.952 [0.928, 0.973]	0.131 [0.111, 0.153]
Non-agreement scorer	0.865 [0.844, 0.885]	0.952 [0.849, 1.000]	0.028 [0.014, 0.044]
BioConCal logistic	0.891 [0.871, 0.910]	0.931 [0.895, 0.961]	0.539 [0.499, 0.578]
BioConCal GBT	0.910 [0.892, 0.928]	0.939 [0.908, 0.966]	0.592 [0.559, 0.626]

Table 19: Document-level bootstrap 95% confidence intervals on the seed-42 test fold (2,000 resamples). The BioConCal-GBT AUROC interval does not overlap the raw-agreement interval. Source: `scripts/bootstrap_doclevel_ci.py, tables/bootstrap_doclevel_ci.csv`.

Correctness key	Cand.	Prev.	Ceiling	AUROC	P@95	R _{cand}	R _{corpus}	Sel. (FP)
Normalized text + type	3,866	0.549	0.883	0.910	0.939	0.592	0.523	1,340 (82)
Exact surface + type	3,866	0.548	0.882	0.912	0.937	0.605	0.534	1,369 (86)
Exact span + type	3,866	0.098	0.158	0.858	1.000	0.032	0.005	12 (0)

Table 20: Candidate keying ablation on the document-level 60/20/20 test fold. The correctness key that labels a candidate as positive is varied while the candidate set and gold-free features are held fixed, and BioConCal-GBT is retrained for each key with a validation-selected 0.95 precision threshold. The occurrence-aware normalized row reproduces the canonical Full-8 result. Exact-surface keying is nearly identical, while exact-span keying collapses the positive set and the ceiling because LLM-emitted offsets are unreliable, which is why exact localization is handled by deterministic alignment rather than as a scoring target. Source: `tables/candidate_keying_ablation.csv`.

Candidate key	Cands	Prev.	Ceiling	AUROC	Raw AUROC	P@0.95
A. normalized-collapsed	12123	0.471	0.470	0.908	0.836	0.958
B. surface key	12580	0.483	0.505	0.911	0.833	0.945
C. occurrence-aware (current)	18812	0.593	0.856	0.910	0.753	0.939
D. relaxed-overlap label	18812	0.758	0.856	0.862	0.745	0.943

Table 21: Candidate keying / granularity ablation. Variant C is the occurrence-aware canonical setting.

I.1 Candidate keying / granularity ablation

The candidate master is occurrence-level: 18,812 rows over 15,611 distinct (`doc`, `type`, `normalized_text`) keys on the four main datasets. The table is a multiset, so repeated mentions and surface variants are kept as distinct rows and not silently merged. If a document mentions *misoprostol* four times and the panel emits the surfaces *misoprostol* and *Misoprostol*, these become separate candidate rows that share the key (`misoprostol`, `chemical`) but differ in surface form and occurrence index; each carries its own surface features while agreement is computed per occurrence. Boundary and granularity variants such as *IL-2* versus *IL-2 receptor* normalize to different keys and remain distinct candidates. Across the four main datasets, roughly one row in six is a repeated-mention or surface-variant occurrence rather than a new normalized identity.

Table 21 varies the candidate key on the document-level test fold (seed 42) and re-trains BioConCal-GBT. Variants A and B collapse to one row per normalized key and per surface key respectively (representative occurrence with the highest agreement count; gold-positive if any occurrence is); C is the occurrence-aware table actually used; D scores the same rows against the relaxed-overlap label. Coverage is occurrence-level against the same corpus gold ($G_{\text{corpus}} = 2,404$). Variant C reproduces the canonical Full-8 numbers (AUROC 0.910, selected 1,340), a no-fabrication check. AUROC and the lift over raw agreement are stable across keys, so the triage conclusion does not depend on the keying scheme; what changes is the occurrence-level ceiling (collapsing repeated mentions lowers recoverable gold occurrences from 0.856 to 0.470), a reporting-granularity effect, not a scorer failure. Source: `scripts/candidate_keying_ablation.py`, `tables/candidate_keying_ablation.csv`.

J Full LODO failure analysis

Deployment checklist. Before applying BioConCal to a new corpus we recommend the fol-

Held-out	Types in test	Unseen-in-train	Prev.	Raw AUROC	GBT AUROC	Log. AUROC	P@95 test	R _{cand} @95 test
BC5CDR	chem., disease	chem.	0.653	0.737	0.781	0.846	1.000	0.001
NCBI Disease	disease	—	0.506	0.869	0.910	0.919	0.979	0.100
BC2GM	gene	gene	0.406	0.766	0.857	0.828	0.771	0.415
JNLPBA	protein, DNA, RNA, cell line, cell type	DNA, RNA, cell line, cell type	0.399	0.794	0.853	0.837	0.889	0.165

Table 22: Full LODO per-fold table, separating ranking transfer (raw and BioConCal AUROC) from operating-point transfer (P@95 and R_{cand}@95 from a source-selected threshold). “Unseen-in-train” lists entity types in the held-out fold but not in training. Sources: `tables/lodo_ranking_vs_threshold_transfer.csv`, `tables/lodo_failure_analysis.csv`.

lowing steps. (1) Verify that the target entity types are represented in the validation data. (2) Estimate the target-domain candidate positive prevalence. (3) Select operating thresholds on target-domain validation documents. (4) Report empirical precision on a held-out target set before use. (5) Use scores for triage only, not for automatic database insertion. (6) If target entity types are unseen in training or calibration, treat a source-selected 0.95-precision threshold as invalid.

K LODO target-domain recalibration

L Gain decomposition

Panel	Features	AUROC	P@95	R _{full} @95
Best open	NA	0.880	0.933	0.262
Closed-2	NA	0.794	0.955	0.160
Closed-2	NA+AG	0.806	0.943	0.286
Open-6	NA	0.899	0.944	0.331
Open-6	NA+AG	0.908	0.958	0.335
Full-8	NA	0.865	0.952	0.028
Full-8	AG	0.873	0.951	0.387
Full-8	NA+AG	0.910	0.939	0.592

Table 24: Gain decomposition on the document-level 60/20/20 test fold. NA is the non-agreement feature block; AG is the agreement-structure block. Source: `tables/gain_decomposition.csv`.

Held-out	n_{cal}	Test P@95	Test $R_{cand}@95$	Sel.	Notes
BC5CDR	0	1.000	0.001	5	source-val (canonical v3 LODO)
BC5CDR	25	0.859 ± 0.100	0.004 ± 0.003	45	target-cal, 3 seeds
BC5CDR	50	0.828 ± 0.063	0.005 ± 0.003	46	target-cal, 3 seeds
BC5CDR	100	0.862 ± 0.090	0.003 ± 0.002	30	target-cal, 3 seeds
NCBI Disease	0	0.979	0.100	47	source-val (canonical v3 LODO)
NCBI Disease	25	0.924 ± 0.007	0.682 ± 0.033	319	target-cal, 3 seeds
NCBI Disease	50	0.904 ± 0.030	0.719 ± 0.086	323	target-cal, 3 seeds
NCBI Disease	100	0.890 ± 0.037	0.737 ± 0.105	291	target-cal, 3 seeds
BC2GM	0	0.771	0.415	280	source-val (canonical v3 LODO)
BC2GM	25	0.830 ± 0.023	0.079 ± 0.080	47	target-cal, 3 seeds
BC2GM	50	0.555 ± 0.393	0.019 ± 0.014	10	target-cal, 3 seeds
BC2GM	100	0.544 ± 0.384	0.019 ± 0.014	9	target-cal, 3 seeds
JNLPBA	0	0.889	0.165	199	source-val (canonical v3 LODO)
JNLPBA	25	0.875 ± 0.008	0.296 ± 0.099	345	target-cal, 3 seeds
JNLPBA	50	0.867 ± 0.009	0.240 ± 0.132	268	target-cal, 3 seeds
JNLPBA	100	0.903 ± 0.028	0.066 ± 0.045	64	target-cal, 3 seeds

Table 23: LODO with target-domain recalibration. The $n_{cal}=0$ rows are canonical source-validation LODO results; $n_{cal} \geq 25$ rows reuse the same source-trained model, select the P95 threshold on target-domain calibration documents, and evaluate on the remaining target documents. Mean \pm sd over three seeds. Source: tables/lodo.target recalibration.summary.csv.

M Full cheap-panel baseline table

N End-to-end interpretation

O Reliability diagram

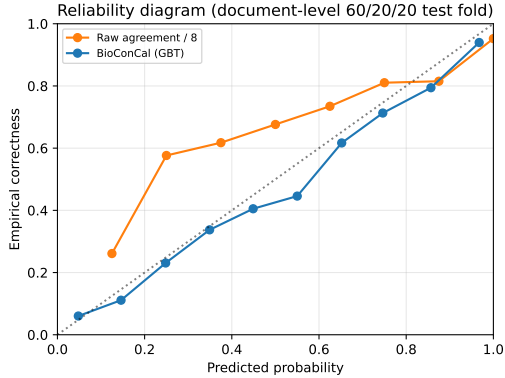


Figure 5: Reliability diagram on the document-level 60/20/20 test fold.

P Agreement-count calibration curve

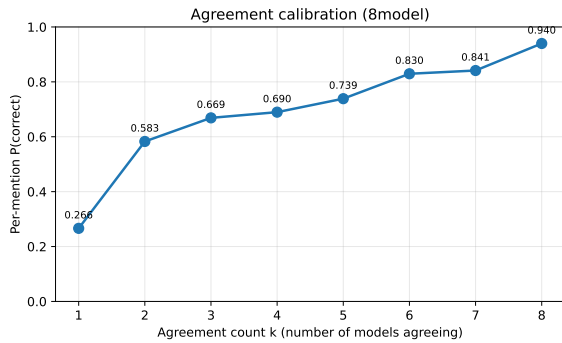


Figure 6: Per-mention $P(\text{correct} | k)$ as a function of agreement count k on the 8-model panel. Precision rises monotonically from 0.266 at $k=1$ to 0.940 at $k=8$.

Q Full selective and conformal baselines

R Panel composition ablation

S Unanimous false-positive audit (auto-suggested)

Auto-suggested category	Count	%
Confirmed false positive	0	0.0
Boundary mismatch	66	73.3
Type confusion	7	7.8
Alias / synonym not in gold	13	14.4
Broader / narrower concept	0	0.0
Possible gold omission	3	3.3
Multiset overflow	1	1.1
Total	90	100.0

Table 30: Auto-suggested category distribution for the 90 unanimous (8-model) false positives. Categories are assigned by a rule-based heuristic and have not been manually verified. “Multiset overflow” is the case where the panel emitted the same (normalized text, type) key more times than gold contained. We also release a 50-case stratified manual-audit sample (audit/unanimous_fp_manual_sample.50.csv) with blank manual_category and manual_notes columns.

T Feature robustness ablation

U Curator workload trade-off

V Learned-selector baselines

W Span alignment per selection rule

Selection rule	Stage	P	R	F1
OpenAI alone	before	0.075	0.077	0.076
OpenAI alone	after	0.765	0.789	0.777
Claude alone	before	0.188	0.143	0.162
Claude alone	after	0.819	0.623	0.708
MiniMax-M2 alone	before	0.019	0.013	0.015
MiniMax-M2 alone	after	0.509	0.332	0.402
Unanimous ($k=8$)	after	0.924	0.113	0.201
BioConCal @ P=0.95	after	0.666	0.175	0.277

Table 34: Exact-span F1 before and after deterministic span realignment. Source: tables/span_alignment_results.csv.

X Open-weight prompt sensitivity

We evaluated prompt sensitivity on a fixed 50-document-per-dataset subset (seed 42) of the four main datasets. The complete three-model open-weight panel used for the cross-prompt agreement-calibration analysis is Phi-4 14B, Mistral-Small 3.2 24B, and MiniMax-M2 230B; these three models ran all three prompts to completion. Llama 3.3 70B (served via Ollama) finished only the original prompt and is therefore

Panel	$ M $	Cand.	Prev.	AUROC	AUPRC	Brier	ECE	Sel.	FP	Test P	Cand. R	Cand. Cov
OpenAI	1	12,628	0.793	0.815	0.937	0.134	0.057	368	6	0.984	0.177	0.141
Claude	1	9,324	0.831	0.814	0.945	0.116	0.065	604	18	0.970	0.373	0.317
Best open	1	7,979	0.674	0.880	0.916	0.134	0.062	596	40	0.933	0.516	0.352
Closed-2	2	13,698	0.769	0.806	0.915	0.140	0.063	644	37	0.943	0.278	0.224
Diverse-3	3	15,156	0.687	0.880	0.926	0.131	0.046	1,003	56	0.944	0.490	0.338
Open-6	6	14,474	0.564	0.908	0.914	0.125	0.055	742	31	0.958	0.458	0.247
Full-8	8	18,812	0.593	0.910	0.923	0.119	0.032	1,340	82	0.939	0.592	0.347

Table 25: Full cheap-panel baseline results on the document-level 60/20/20 test fold. Prev. is positive prevalence in the panel candidate universe. Sel., FP, and Test P are at the validation-selected P95 operating point. Test P is empirical test precision. Cand. R and Cand. Cov are candidate recall and candidate coverage over the panel’s own universe. The main-text Table 4 reports $R_{full}@95$, which is recall over the full eight-panel positive candidate set. Source: tables/single_model_candidate_baselines_p95.csv.

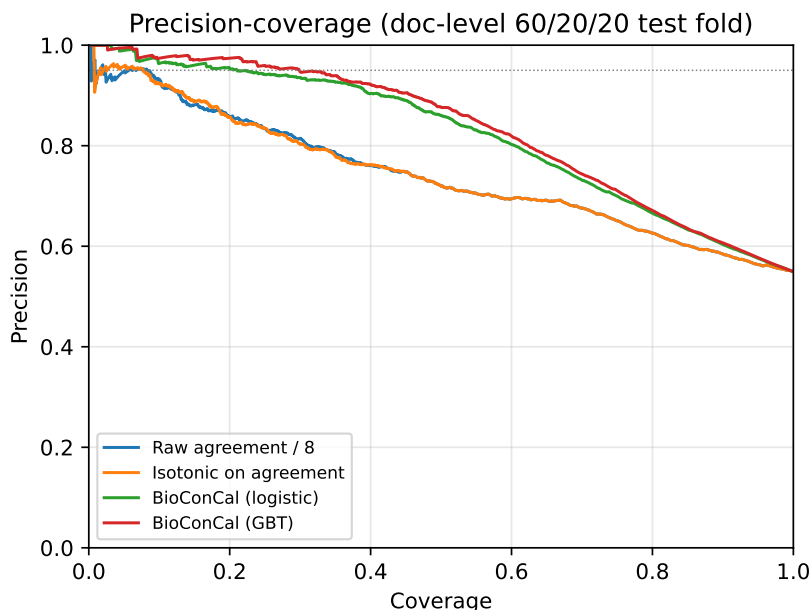


Figure 7: Precision-coverage curves on the document-level 60/20/20 test fold. BioConCal improves on raw agreement count across the coverage range.

Method	Sel.	FP	C-P	C-R	Corp-R
Union (any model)	3,866	1,742	0.549	1.000	0.883
OpenAI \cup Claude	2,743	743	0.729	0.942	0.832
Agree ≥ 2	2,587	797	0.692	0.843	0.745
Agree ≥ 4	1,275	260	0.796	0.478	0.422
Agree ≥ 6	715	93	0.870	0.293	0.259
Unanimous ($k=8$)	293	14	0.952	0.131	0.116
BioConCal P95	1,340	82	0.939	0.592	0.523

Table 26: End-to-end interpretation on the doc-level 60/20/20 test fold. C-P is candidate precision. C-R is candidate recall (selected TP over 2,124 gold-positive candidates). Corp-R is corpus-level recall (selected TP over 2,404 gold mentions in the test corpus). The empirical union candidate recall is 0.883, which caps Corp-R for any candidate-level method. Source: tables/end_to_end_interpretation.csv.

partial; it contributes to the single-model table for the original prompt but is excluded from the cross-prompt agreement calibration to keep the panel size constant across prompts. CHEMDNER is excluded from this analysis because the main paper already treats it as robustness-only (its public mirror does not provide reliable character offsets). These results are not claimed as closed-model robustness or as full eight-model prompt sensitivity; closed-API models (OpenAI GPT-5.5 and Claude Opus 4.7) were not re-run with prompt variants. Three prompts are compared: *original_zero_shot* (the main paper’s template), *strict_entity_only* (instructs the model to extract only explicit surface mentions and not infer entities), and *few_shot_2_examples* (two synthetic illustrative examples that do not overlap the evaluation subset).

Workflow	Cand. source	Test P	TP	FP	Sel.	R_{corpus}	Triage fit	Main interpretation
Unanimous / raw agree- ment P95	LLM-8	0.952	279	14	293	0.116	Low yield	High precision, but too conservative for review yield
Agreement ≥ 2	LLM-8	0.692	1,790	797	2,587	0.745	Low precision	High raw recall, but 797 FPs make the queue noisy
BERN2 take-all	BERN2	0.806	1,772	427	2,199	0.737	Unfiltered	Higher coverage, but no learned candidate filter
LLM-8 \cup BERN2 ex- ploratory merge	additive union	0.836	1,323	260	1,583	0.550	Unfiltered	Raises ceiling, but unfiltered additions add FPs
BioConCal GBT	LLM-8	0.939	1,258	82	1,340	0.522	Primary	Largest primary high precision review yield
BioConCal-Hybrid	merged union	0.929	1,716	131	1,847	0.709	Tradeoff	Higher coverage, but lower precision than LLM-8 BioConCal

Table 27: Curator triage utility under high precision review constraints on the document level test fold. Rows compare fixed voting, unfiltered source expansion, and learned scoring workflows by empirical precision and selected yield. The primary BioConCal operating point is selected on validation at the 0.95 precision target. TP denotes selected candidate row positives. Hybrid R_{corpus} uses multiset corpus accounting, with 1,705 selected gold occurrences over 2,404 corpus gold mentions. BioConCal GBT is the primary LLM-8 review queue. BioConCal-Hybrid scores the expanded LLM-8 \cup BERN2 universe and trades precision for coverage. This is a curator triage comparison, not an end-to-end extraction. Data sources are `tables/risk_control_selection_docsplit.csv`, `tables/end_to_end_interpretation.csv`, `tables/main_candidate_generator_comparison.csv`, and `tables/hybrid_curator_utility.csv`.

Method	Sel.	FP	Test P	Test R	P gap
Raw agreement (val P95)	293	14	0.952	0.131	+0.002
Conformal-style raw cutoff ($\alpha=0.05$)	715	93	0.870	0.293	-0.080
Platt scaling on k	293	14	0.952	0.131	+0.002
Isotonic on k	293	14	0.952	0.131	+0.002
BioConCal GBT (val P95)	1,340	82	0.939	0.592	-0.011
Conformal-style BioConCal cutoff ($\alpha=0.05$)	1,362	83	0.939	0.602	-0.011

Table 28: Selective and split-conformal-inspired baselines on the document-level 60/20/20 split. “P gap” is the empirical test precision minus the 0.95 nominal target. Source: `tables/selective_baselines.csv`. These are comparison baselines, not formal finite-sample precision guarantees.

Panel	N_{cand}	AUROC	Brier	ECE	P@95	$R_{\text{cand}}@95$
All 8 models	18,812	0.910	0.119	0.032	0.939	0.592
Open-weight 6	14,474	0.908	0.142	0.069	0.958	0.458
Closed 2 (OpenAI+Claude)	13,698	0.806	0.211	0.117	0.943	0.278
Drop OpenAI	16,977	0.911	0.121	0.038	0.937	0.632
Drop Claude	18,174	0.909	0.124	0.039	0.933	0.574

Table 29: Panel-composition ablation of BioConCal-GBT under the document-level 60/20/20 split. Agreement features are recomputed from each panel subset; candidates with zero in-panel votes are removed. The closed-only two-model panel drops AUROC to 0.806, consistent with the importance of model diversity. The full leave-one-model-out grid is stable in the 0.899–0.912 AUROC range and is in `tables/panel_composition_ablation.csv`.

Y Per-dataset candidate coverage

Z Per-dataset agreement calibration and normalization

Per-unified-type agreement calibration is released as `tables/agreement_calibration_by_type.csv`.

The normalization ablation comparing exact-surface, normalized, and relaxed-overlap matching is in `tables/normalization_ablation.csv`.

The mean F1 lift from exact-surface to normalized

matching is small across all eight models. The lift from normalized to relaxed-overlap is larger but does not change the model ranking, so the central findings hold under either matching variant.

Variant (GBT)	#feat.	AUROC	Δ AUROC	Brier	P@95	$R_{\text{cand}@95}$	Sel
A. BioConCal main model	19	0.910	+0.000	0.119	0.939	0.592	1,340
B. remove entity_type	18	0.906	-0.004	0.122	0.940	0.559	1,264
C. remove doc_text_length	18	0.909	-0.001	0.119	0.942	0.549	1,238
D. remove surface availability	15	0.910	+0.000	0.120	0.935	0.599	1,361
E. remove offset only	17	0.910	+0.000	0.120	0.935	0.599	1,361
F. remove doc length + surface avail.	14	0.912	+0.002	0.117	0.934	0.600	1,364
G. agreement + mention only	13	0.909	-0.001	0.120	0.941	0.528	1,193
H. agreement only	4	0.860	-0.050	0.149	—	0.000	0
I. vote-pattern only	8	0.859	-0.051	0.151	0.953	0.143	318

Table 31: Feature-removal robustness ablation under the doc-level 60/20/20 split and val-frozen P95 protocol. Δ AUROC is relative to variant A, the main 19-feature BioConCal model. AUROC and $R_{\text{cand}@95}$ are stable across A–G (max $|\Delta$ AUROC| = 0.004); only stripping to agreement-only (H) or vote-pattern-only (I) collapses precision-targeted selection. The non-agreement features (mention/surface/document) are useful in-domain but not the dominant signal, and the scorer is not driven by corpus-specific formatting shortcuts. Source: tables/feature_robustness_ablation.csv.

Method	Sel.	TP	FP	Δ TP	Δ FP	Δ FP/ Δ TP	Reviewed/ Δ TP
Unanimous ($k=8$)	293	279	14	0	0	0	0
BioConCal GBT (val P95)	1,340	1,258	82	979	68	0.069	1.069

Table 32: Curator workload trade-off between Unanimous and BioConCal P95 on the doc-level test fold. “ Δ TP” and “ Δ FP” are gains over Unanimous; “ Δ FP/ Δ TP” is the marginal false-positive cost per additional true candidate; “Reviewed/ Δ TP” is the curator-side review burden per recovered true positive. Source: tables/curator_workload_tradeoff.csv.

Selector	AUROC	Brier	P@95	$R_{\text{cand}@95}$	Sel	FP
Raw agreement threshold	0.753	0.237	0.952	0.131	293	14
Agreement-count logistic	0.753	0.205	0.952	0.131	293	14
Agreement-count GBT	0.751	0.199	0.952	0.131	293	14
Vote-pattern logistic	0.864	0.148	0.941	0.151	341	20
Vote-pattern GBT	0.859	0.151	0.953	0.143	318	15
Agreement-family GBT	0.860	0.149	—	—	0	0
Agreement + mention GBT	0.909	0.120	0.941	0.528	1,193	71
BioConCal GBT (main 19-feature)	0.910	0.119	0.939	0.592	1,340	82

Table 33: Learned-selector baselines under the same doc-level 60/20/20 split and val-targeted P95 protocol. Vote-pattern (8 per-model indicators) and aggregate-agreement (4-feature) GBT classifiers both reach AUROC \approx 0.86 but recover little precision-targeted recall; the largest $R_{\text{cand}@95}$ jump comes from adding mention features. The agreement-family GBT row selects zero candidates because no val-fold operating point of that classifier reaches the 0.95 precision target. Source: tables/learned_selectors_baseline.csv.

Prompt	Cands	P@1	P@2	P@max	Agr.	AUC
original_zero_shot	797	0.251	0.585	0.876	0.778	
strict_entity_only	649	0.392	0.704	0.919	0.742	
few_shot_2_examples	913	0.241	0.589	0.776	0.753	

Table 35: Open-weight prompt sensitivity on the three-model panel (Phi-4, Mistral-Small 3.2, MiniMax-M2; max agreement $k=3$). $P(\text{correct} | k)$ is monotonic in k for all three prompts. Strict prompting raises high-agreement precision at the cost of recall; few-shot prompting raises recall at the cost of P@max k . Source: tables/prompt_sensitivity_summary.csv.

Dataset	Gold	Represented	Ceiling	Union cand	BC Sel	BC Corp-R
BC5CDR	1,939	1,643	0.847	3,398	1,228	0.594
NCBI Disease	108	95	0.880	175	47	0.426
BC2GM	130	105	0.808	184	13	0.069
JNLPBA	227	214	0.943	558	52	0.225
Test total	2,404	2,057	0.856	3,866	1,340	0.523

Table 36: Per-dataset candidate coverage on the doc-level 60/20/20 test fold. “Gold” is the total gold mentions in the test docs; “Represented” counts gold mentions whose (normalized text, type) key appears in the candidate universe. Two numbers can be reported here: the *stricter multiset gold-key coverage* (0.856 total, where a gold mention only counts as represented if a candidate has the same key under multiset bookkeeping), and the *empirical union candidate recall under candidate-level matching* used in the main text (0.883 total). BC (BioConCal) Corp-R is selected TP / dataset gold mentions. Source: tables/candidate_universe_ceiling.csv.

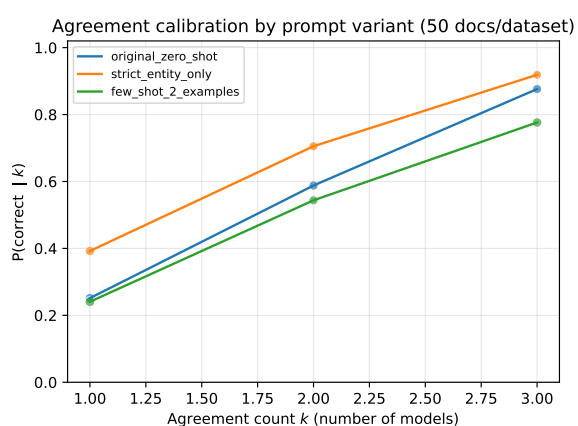


Figure 8: Agreement calibration across the three prompt variants on the open-weight 50-doc-per-dataset subset. Marker size scales with the number of candidates at each agreement count.

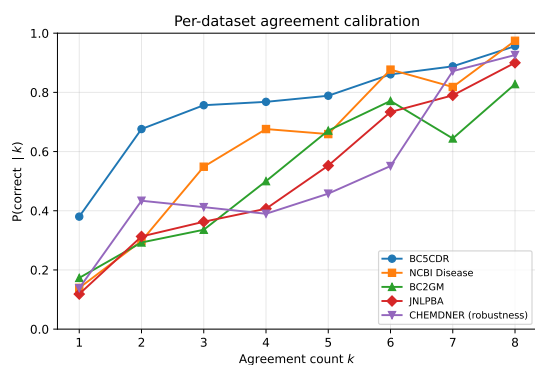


Figure 9: Agreement calibration broken down by dataset. BC5CDR and NCBI Disease reach 0.96 and 0.97 at $k=8$. BC2GM reaches 0.83, JNLPBA reaches 0.90. Source: tables/agreement_calibration_by_type.csv and figures/figure_calibration_by_dataset.pdf.